



OPEN

## Comprehensive exploration of chemical space using trisubstituted carboranes

Yasunobu Asawa<sup>1</sup>, Saki Hatsuzawa<sup>2</sup>, Atsushi Yoshimori<sup>3</sup>, Kentaro Yamada<sup>4,5</sup>, Akira Katoh<sup>5</sup>, Hiroyuki Kouji<sup>6</sup> & Hiroyuki Nakamura<sup>1,7</sup>✉

A total of 42 trisubstituted carboranes categorised into five scaffolds were systematically designed and synthesized by exploiting the different reactivities of the twelve vertices of *o*-, *m*-, and *p*-carboranes to cover all directions in chemical space. Significant inhibitors of hypoxia inducible factor transcriptional activity were mainly observed among scaffold V compounds (e.g., Vi-m, and Vo), whereas anti-rabies virus activity was observed among scaffold V (Va-h), scaffold II (IIb-g), and scaffold IV (IVb) compounds. The pharmacophore model predicted from compounds with scaffold V, which exhibited significant anti-rabies virus activity, agreed well with compounds IIb-g with scaffold II and compound IVb with scaffold IV. Normalized principal moment of inertia analysis indicated that carboranes with scaffolds I-V cover all regions in the chemical space. Furthermore, the first compounds shown to stimulate the proliferation of the rabies virus were found among scaffold V carboranes.

Biomolecules play an important role in maintaining living systems in a crowded biological environment. The structure of biomolecules is three-dimensional, and these molecules interact with each other to construct complex biological networks and systems that comprise robust and redundant functionalities. Dysfunctions of such networks and systems cause diseases, and drugs help restore these networks and systems correct physiological functions. Therefore, drugs need to work in the three-dimensional chemical space of biomolecular interactions. More complex molecules are deemed to have the ability to access a larger chemical space<sup>1,2</sup>, and natural products meet this complexity requirement due to their enormous structural diversity<sup>3,4</sup>. In fact, many small molecular drugs on the market are derived from natural products<sup>5</sup>. Lovering et al. suggested that the higher the fraction of sp<sup>3</sup> carbon centres (Fsp<sup>3</sup>) in a small molecule, the higher the probability that the small molecule will make its way from drug discovery through clinical trials to becoming a drug<sup>6-8</sup>. Diversity-oriented synthesis (DOS), a concept for synthesis to access structurally complex and diverse compounds<sup>9</sup>, has been developed with the goal of producing three-dimensional complex drug-like compounds and chemical modulators<sup>10-14</sup>. However, the systematic design of three-dimensional divergent molecules as a way to explore the chemical space has not been fully investigated yet<sup>8</sup>.

We focused on the icosahedral structure of carborane (dicarba-*closo*-dodecaborane). Notably, carborane consists of two carbon atoms, ten boron atoms, and ten hydrogen atoms, and three different isomers of this species are possible, depending on the relative position of two carbons: *ortho* (1,2), *meta* (1,7), and *para* (1,12)<sup>15,16</sup>. Given its three-dimensional hydrophobic features, over the past two decades, carborane has attracted much attention as a hydrophobic pharmacophore for drug discovery<sup>17-20</sup>. Indeed, by introducing substituents on the carbon centres of carborane, various promising drug candidates have been synthesised, including 17β-estrogen mimics<sup>17,21</sup>, antifolates<sup>22</sup>, HSP60 inhibitors<sup>23,24</sup>, COX-2 inhibitors<sup>25,26</sup>, vitamin D receptor ligands<sup>27,28</sup>, and nicotinamide phosphoribosyl-transferase inhibitors<sup>29,30</sup>. We assumed that, by introducing three substituents at arbitrary carbon positions on carborane, it would be possible to spatially cover all directions. In fact, five types

<sup>1</sup>School of Life Science and Technology, Tokyo Institute of Technology, 4259, Nagatsuta-cho, Midori-ku, Yokohama 226-8503, Japan. <sup>2</sup>School of Science, Kitasato University, 1-15-1, Kitazato, Minami-ku, Sagami-hara-shi, Kanagawa 252-0373, Japan. <sup>3</sup>Institute for Theoretical Medicine, Inc., 26-1, Muraoka-Higashi 2-Chome, Fujisawa, Kanagawa 251-0012, Japan. <sup>4</sup>Faculty of Agriculture, Miyazaki University, 1-1, Gakuenkibanadai-Nishi, Miyazaki 889-2192, Japan. <sup>5</sup>Faculty of Medicine, Oita University, 1-1, Idaigaoka, Hasama-machi, Yufu-City, Oita 879-5593, Japan. <sup>6</sup>Oita University Institute of Advanced Medicine, Inc., 17-20, Higashi Kasuga-machi, Oita City, Oita 870-0037, Japan. <sup>7</sup>Laboratory for Chemistry and Life Science, Institute of Innovative Research, Tokyo Institute of Technology, 4259, Nagatsuta-cho, Midori-ku, Yokohama, Kanagawa 226-8503, Japan. ✉email: hiro@res.titech.ac.jp

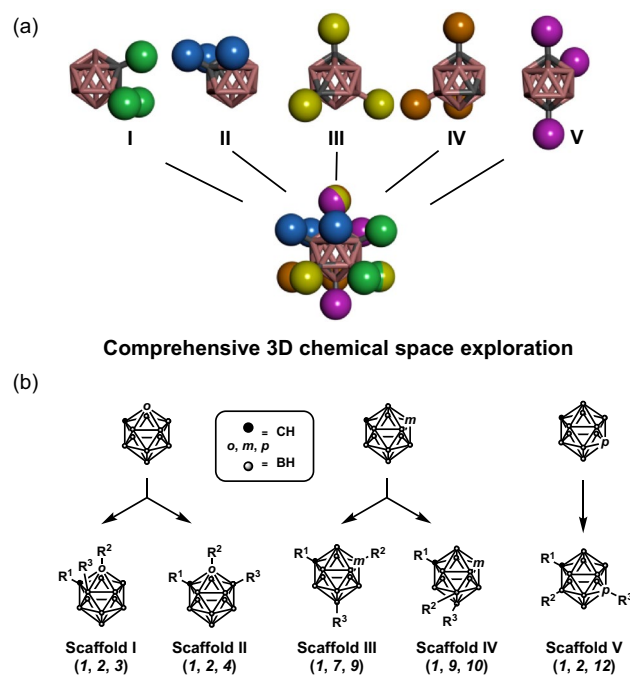


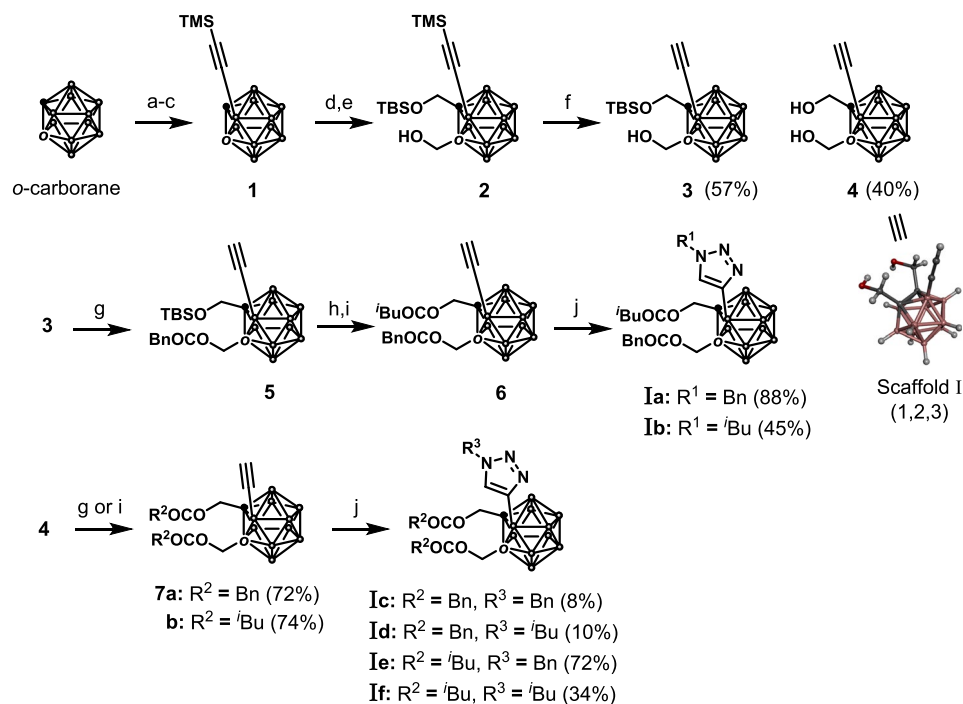
**Figure 1.** (a) The five types of trisubstituted carboranes that can cover all directions in a chemical space. (b) Synthetic strategy for the production of the described trisubstituted carboranes.

of trisubstituted carboranes can be designed that satisfy all directions in a chemical space, as can be evinced from Fig. 1a. Since the twelve vertices of carborane have mutually different reactivities, it should be possible to design different synthetic approaches to producing the various trisubstituted carboranes<sup>31,32</sup>. Although a limited number of trisubstituted carboranes has been reported<sup>31</sup>, the systematic design of trisubstituents undertaken to achieve the DOS for the development of drug candidates has not yet been investigated. In the present study, we synthesised five types of trisubstituted carboranes: scaffolds I and II from *o*-carborane, scaffolds III and IV from *m*-carborane, and scaffold V from *p*-carboranes (Fig. 1b).

## Results and discussion

**Synthesis of trisubstituted carboranes.** We developed tricyclic three-dimensional scaffolds that are rich in  $sp^3$ -hybridized carbon centres to access unexplored chemical spaces, and we used these scaffolds to design peptidomimetic molecules<sup>33–35</sup>. The  $\alpha$ -helix is one of the important elements of a protein's secondary structure that affords the construction of three-dimensional tertiary structures of proteins. It is also a structure found in many protein–protein interactions (PPIs)<sup>36</sup>, and the  $\alpha$ -helix plays an important role in biological networks<sup>37–39</sup>. Although PPIs have been attracting the attention of researchers as drug targets, their contact surfaces are relatively large (750–1500 Å<sup>2</sup>)<sup>36,40</sup> compared with their counterparts between proteins and small molecules (~300 Å<sup>2</sup>)<sup>41</sup>. Therefore, the development of small molecule inhibitors targeting PPIs remains a challenging proposition. Recently, the FDA approved Venetoclax (ABT-199)<sup>42</sup> as a first-in-class small molecule-based PPI inhibitor targeting the Bcl-2/Bax interaction<sup>43,44</sup>. The X-ray co-crystal structure of Bcl-x<sub>L</sub>/Bax with ABT-737 revealed that ABT-737 binds in the same cleft as the Bax native helix at the Bcl-x<sub>L</sub>/Bax interface<sup>37,45</sup>. The protein–protein interfaces usually contain crucial residues for the PPI called ‘hot spots’<sup>46</sup>, which are often composed of hydrophobic amino acid residues<sup>47,48</sup>. In this study, benzyl (Bn) and isobutyl (iBu) groups were introduced into the carborane scaffolds as mimics of hydrophobic amino acid residues phenylalanine and leucine, respectively<sup>34</sup>.

The approach to the synthesis of scaffold I (1,2,3-trisubstituted *o*-carboranes) implemented in this study is detailed in Scheme 1. We were concerned that a direct amide bond to the *o*-carborane cluster could cause degradation via deboronation induced by the amide group<sup>26</sup>. Therefore, *o*-carborane was functionalized without introducing any amide bonds. Selective iodination at the 3-position of *o*-carborane was performed according to a literature procedure<sup>49</sup>, and the resulting B3-iodocarborane was subjected to the Kumada–Tamao–Corriu cross coupling to produce **1** in 70% yield<sup>50</sup>. After the lithiation on C1 of **1** with <sup>t</sup>BuLi followed by the addition to paraformaldehyde, the resulting hydroxy group was protected with the *tert*-butyldimethylsilyl (TBS) group. The modification of another hydroxy methyl group on C2 achieved in the same manner described for C1 afforded compound **2**. Removing the trimethylsilyl (TMS) group of **2** with potassium carbonate produced a mixture of mono-alcohol **3** and di-alcohol **4** in 57% and 40% yields, respectively. Notably, the structure of **4** was unambiguously determined by X-ray structural analysis. Esterification of **3** with phenylacetyl chloride gave compound **5** in 46% yields over two steps. The TBS group was then removed, and the resulting alcohol was esterified with isovaleryl chloride to afford compound **6** in 90% yields over two steps. Finally, acetylene **6** was subjected to a Huisgen cycloaddition reaction with benzyl azide or isobutyl azide in the presence of CuI and sodium ascorbate

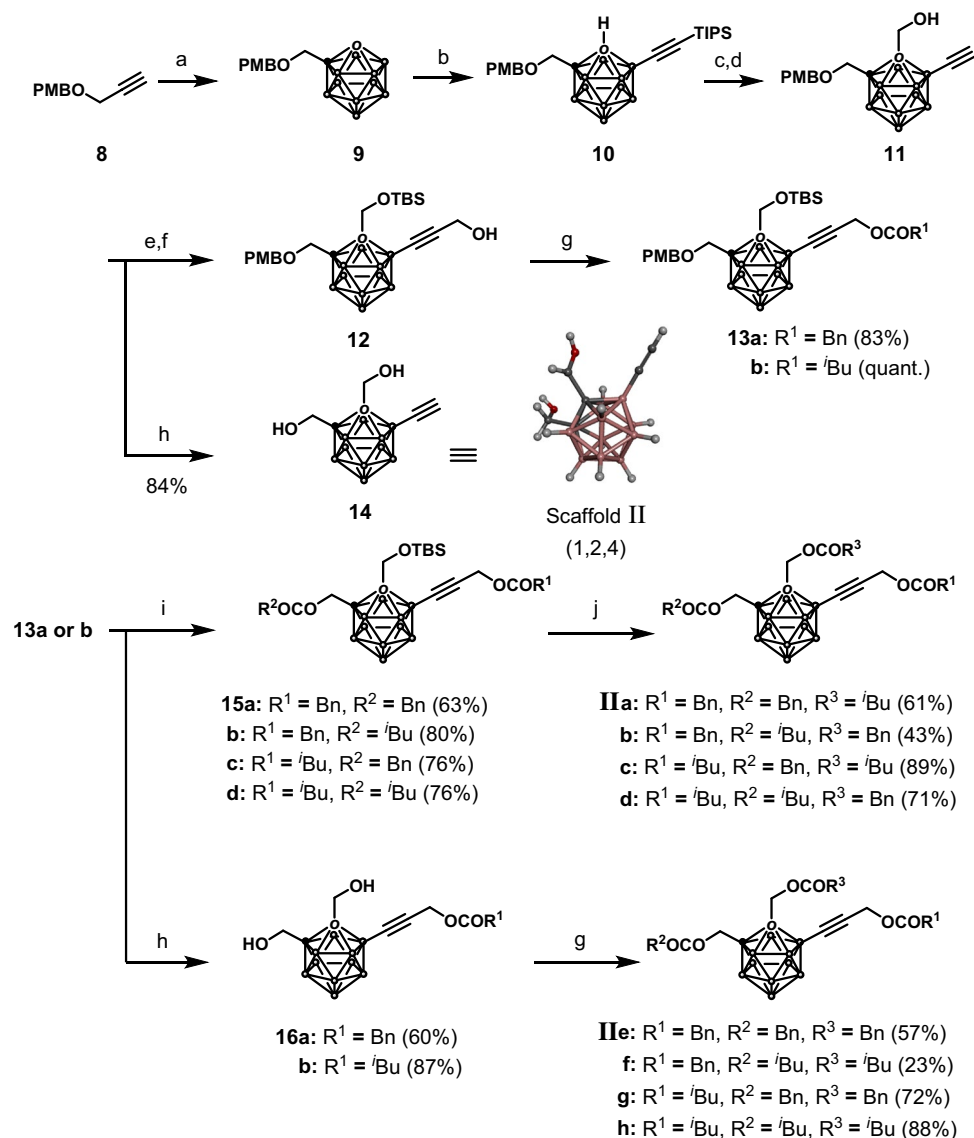


**Scheme 1.** Synthesis of 1,2,3-trisubstituted *o*-carboranes (scaffold I). Reaction conditions: (a) KF, ethanol, reflux; then, HCl, (CH<sub>3</sub>)<sub>3</sub>NHCl, r.t., 87%; (b) <sup>n</sup>BuLi, diethyl ether, r.t.; then, BI<sub>3</sub>, toluene, r.t., 81%; (c) TMSC<sub>2</sub>MgBr, Pd(PPh<sub>3</sub>)<sub>2</sub>Cl<sub>2</sub>, THF, 80 °C, 70%; (d) (i) <sup>n</sup>BuLi, (CHO)<sub>n</sub>, THF, -78 °C to 0 °C; (ii) TBSOTf, 2,6-lutidine, CH<sub>2</sub>Cl<sub>2</sub>, 0 °C to r.t., 20% in two steps; (e) <sup>n</sup>BuLi, (CHO)<sub>n</sub>, THF, -78 °C to 0 °C, 20%; (f) K<sub>2</sub>CO<sub>3</sub>, methanol, r.t.; (g) BnCOCl, Et<sub>3</sub>N, CH<sub>2</sub>Cl<sub>2</sub>, r.t., 81%; (h) HCl-dioxane, CH<sub>2</sub>Cl<sub>2</sub>, r.t., 90%; (i) <sup>t</sup>BuCOCl, Et<sub>3</sub>N, CH<sub>2</sub>Cl<sub>2</sub>, r.t., quant.; (j) BnN<sub>3</sub> or <sup>i</sup>BuN<sub>3</sub>, CuI, Na-ascorbate, DMF/H<sub>2</sub>O, r.t.; TMS: trimethylsilyl; TBS: *tert*-butyldimethylsilyl; Bn: benzyl; <sup>i</sup>Bu: isobutyl; DMF: dimethylformamide; Et: ethyl; PPh<sub>3</sub>: triphenylphosphine; r.t.: room temperature; OTf: triflate.

to obtain the trisubstituted carboranes **1a** and **1b** in 45% and 88% yields, respectively. On the other hand, esterification of two hydroxy groups on **4** with the identical substituents afforded **7a** and **7b** in 72% and 74% yields, respectively; subjecting **7a** and **7b** to the Hüsgen cycloaddition reaction with benzyl azide or isobutyl azide gave **Ic–f** in yields ranging between 8 and 72%. Thus, the synthesis of 1,2,3-trisubstituted carboranes with different substituents on the three tethers was achieved in scaffold I.

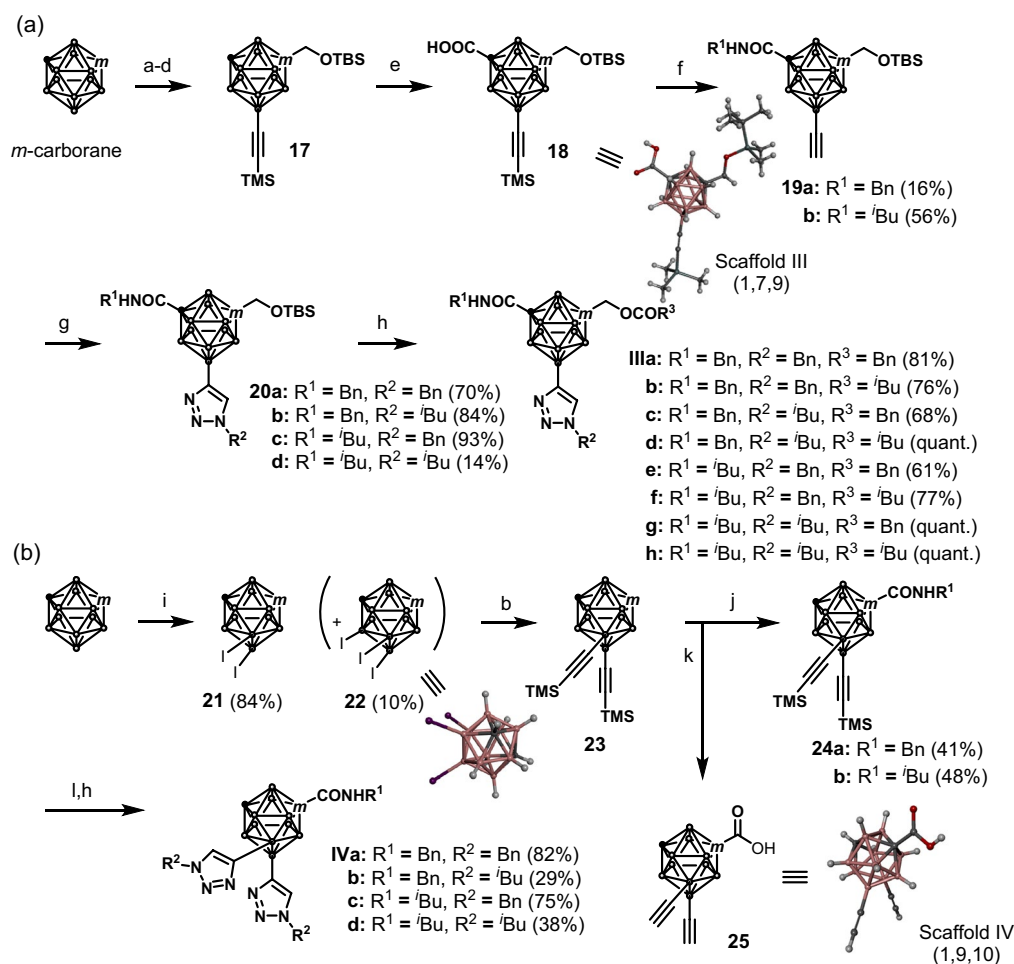
Next, the synthesis of scaffold II (1,2,4-trisubstituted *o*-carboranes) was carried out according to the approach detailed in Scheme 2. Propargyl *p*-methoxybenzyl (PMB) ether (**8**) was made to react with decaborane in the presence of *N,N*-dimethylaniline under microwave (MW) irradiation in chlorobenzene to obtain the 1-substituted *o*-carborane **9** in 79% yield<sup>51</sup>. A carboxylic acid moiety was then introduced into the C2-position of **9** using <sup>n</sup>BuLi and carbon dioxide, which functioned as a directing group to afford the selective alkylation of the B4-position via an approach developed by Xie and co-workers, producing compound **10** in 31% yield over two steps<sup>31</sup>. Notably, the carboxylic acid intermediate had to be immediately subjected to the alkylation reaction to avoid the deprotection of the PMB group induced by the acidity of the intermediate. After introducing a hydroxy methyl group into the C2-position of compound **10** via an approach similar to that of step d in Scheme 1, the triisopropylsilyl (TIPS) group of the alkyne moiety was removed. The TBS protection of the hydroxy group of compound **11**, followed by the introduction of a hydroxy methyl group into the terminal alkyne, afforded compound **12**. The hydroxy group on compound **12** was converted into either a Bn group (**13a**, 83% yield) or an <sup>i</sup>Bu group (**13b**, quant.). On the other hand, removal of the PMB group of compound **11** afforded dialcohol **14**, whose structure was determined by X-ray structural analysis. (It should be noted that good quality crystals even made several measurements were not obtained due to the unnecessary reflections.). The PMB group of compound **13** was selectively removed using 2,3-dichloro-5,6-dicyano-*p*-benzoquinone (DDQ), and the subsequent esterification of the deprotected derivatives of compounds **13a** and **13b** with phenylacetyl chloride or isovaleryl chloride afforded compounds **15a–d**. After removing the TBS group, Bn and <sup>i</sup>Bu groups were introduced into the C2-position of **15** to obtain the 1,2,4-trisubstituted carboranes **11a–d** in 43–89% yields. Furthermore, compounds **13a** and **13b** were treated with HCl in dioxane, and Bn and <sup>i</sup>Bu groups were introduced into the resulting diols **16** to obtain compounds **11e–h** in 23–88% yields.

Next, we synthesized 1,7,9-substituted carboranes (scaffold III) and 1,9,10-substituted carboranes (scaffold IV) using *m*-carborane as the starting building block (Scheme 3). Selective electrophilic iodination at the B9-position of *m*-carborane followed by the Kumada–Tamao–Corriu cross coupling were performed implementing a literature procedure<sup>50</sup>. A hydroxy methyl group was then introduced into the C1 position of the resulting 9-(trimethylsilyl)ethynyl)-*m*-carborane in a similar manner to that described for the synthesis of compounds **1**



**Scheme 2.** Synthesis of 1,2,4-trisubstituted *o*-carboranes (scaffold II). Reaction conditions: (a) B<sub>10</sub>H<sub>14</sub>, *N,N*-dimethylaniline, PhCl, 130 °C, MW, 79%; (b) (i) <sup>n</sup>BuLi, CO<sub>2</sub>, diethyl ether, -78 °C to r.t.; (ii) TIPSC≡CH, Pd(OAc)<sub>2</sub>, AgOAc, K<sub>2</sub>HPO<sub>4</sub>, toluene, 80 °C, 31% in two steps; (c) <sup>n</sup>BuLi, (CHO)<sub>n</sub>, THF, -78 °C to 0 °C, 80%; (d) TBAF, THF, 0 °C, quant.; (e) TBSOTf, 2,6-lutidine, CH<sub>2</sub>Cl<sub>2</sub>, 0 °C to r.t., 98%; (f) <sup>n</sup>BuLi, (CHO)<sub>n</sub>, THF, -78 °C to 0 °C, 79%; (g) BnCOCl or <sup>i</sup>BuCOCl, Et<sub>3</sub>N, CH<sub>2</sub>Cl<sub>2</sub>, r.t.; (h) DDQ, NaH<sub>2</sub>PO<sub>4</sub>, CH<sub>2</sub>Cl<sub>2</sub>-H<sub>2</sub>O, r.t.; (i) i—DDQ, NaH<sub>2</sub>PO<sub>4</sub>, CH<sub>2</sub>Cl<sub>2</sub>-H<sub>2</sub>O, r.t., ii—BnCOCl or <sup>i</sup>BuCOCl, Et<sub>3</sub>N, CH<sub>2</sub>Cl<sub>2</sub>, r.t.; (j) i—HCl-dioxane, CH<sub>2</sub>Cl<sub>2</sub>, r.t.; ii—BnCOCl or <sup>i</sup>BuCOCl, Et<sub>3</sub>N, CH<sub>2</sub>Cl<sub>2</sub>, r.t.. Bn: benzyl; Bu: butyl; Et: ethyl; <sup>i</sup>Bu: isobutyl; OAc: acetate; Ph: phenyl; OTf: triflate; PMB: *p*-methoxybenzyl; MW: microwave irradiation; TIPS: triisopropylsilyl; TBAF: tetrabutylammonium fluoride; TBS: *tert*-butyldimethylsilyl; DDQ: 2,3-dichloro-5,6-dicyano-*p*-benzoquinone; r.t.: room temperature.

to **2** (see Scheme 1), followed by TBS protection to give the 1,9-disubstituted *m*-carborane **17** in 42% yield over four steps. Afterwards, a carboxylic acid group was introduced into the C7-position of compound **17** using <sup>n</sup>BuLi and carbon dioxide, and the resulting carboxylic acid **18** was subjected to amidation with either benzyl amine or isobutyl amine in the presence of 1-(3-dimethylaminopropyl)-3-ethylcarbodiimide hydrochloride (EDCI), 1-hydroxybenzotriazole monohydrate (HOBt), and *N,N*-diisopropylethylamine (DIEA); the subsequent removal of the TMS group afforded compounds **19a** and **19b** in 16% and 55% yields over two steps, respectively. These two compounds were then subjected to Hüsgen cycloaddition reactions with benzyl azide or isobutyl azide implementing the approach detailed in Scheme 1 to give compounds **20a–d** in 14–93% yields. Finally, removal of the TBS group followed by an esterification process afforded 1,7,9-substituted carboranes **IIa–h** in 61% to quantitative yields over two steps. Scaffold IV was obtained according to the synthetic procedure depicted in Scheme 3b. The selective electrophilic diiodination at the 9,10-positions of *m*-carborane was achieved under microwave

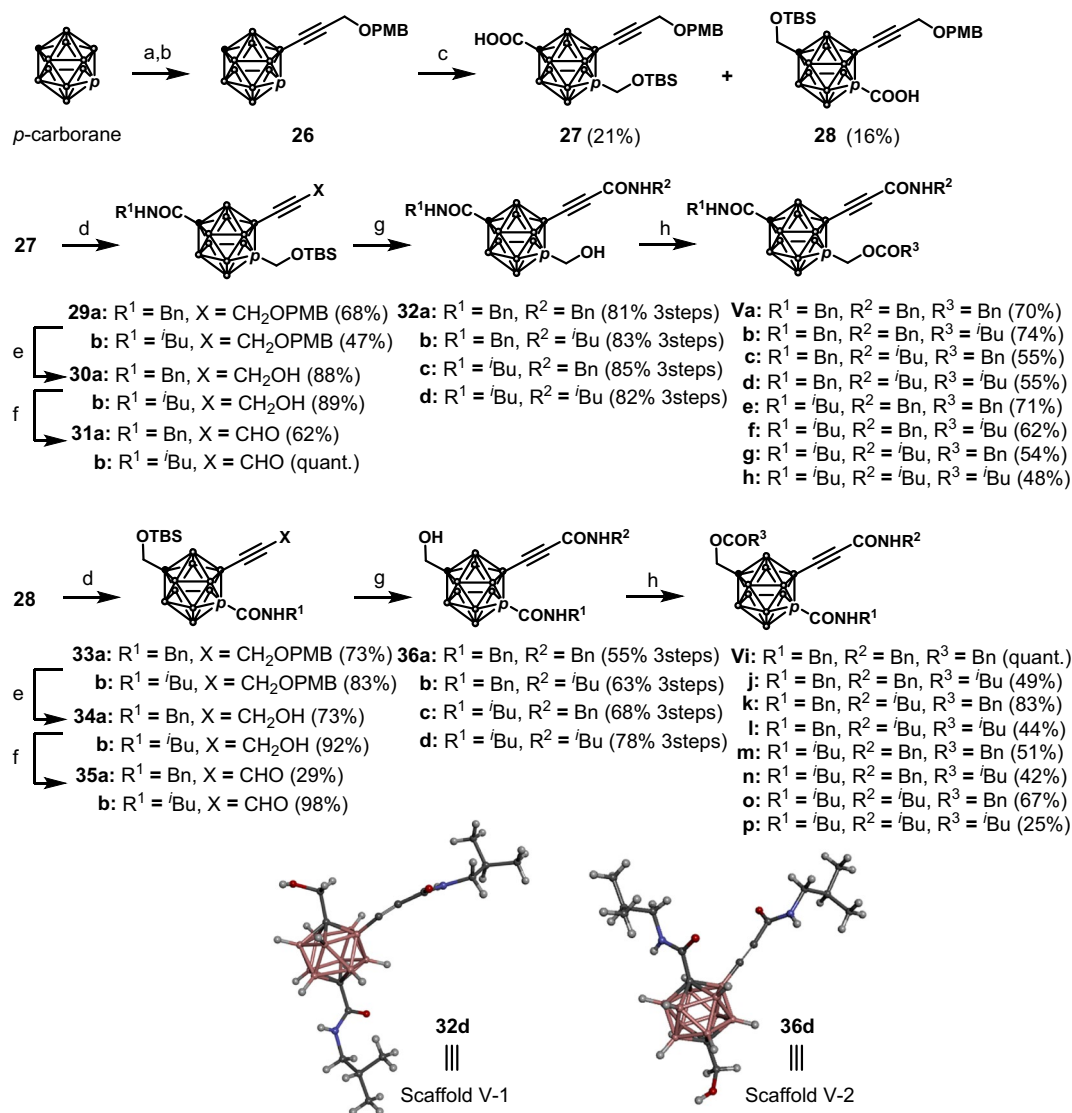


**Scheme 3.** Syntheses of 1,7,9-substituted carboranes (scaffold III) (a) and 1,9,10-substituted carboranes (scaffold IV) (b). Reaction conditions: (a) I<sub>2</sub>, AlCl<sub>3</sub>, CH<sub>2</sub>Cl<sub>2</sub>, r.t., 96%; (b) TMSC<sub>2</sub>MgBr, Pd(PPh<sub>3</sub>)<sub>2</sub>Cl<sub>2</sub>, THF, 80 °C, 96%; (c) <sup>n</sup>BuLi, (CHO)<sub>n</sub>, THF, -78 °C to 0 °C, 46%; (d) TBSOTf, 2,6-lutidine, CH<sub>2</sub>Cl<sub>2</sub>, 0 °C to r.t., 99%; (e) <sup>n</sup>BuLi, CO<sub>2</sub>, THF, -78 °C to r.t., 92%; (f) i—EDCI, HOBT, DIEA, BnNH<sub>2</sub>, or <sup>i</sup>BuNH<sub>2</sub>, THF, r.t.; ii—K<sub>2</sub>CO<sub>3</sub>, methanol, r.t.; (g) BnN<sub>3</sub> or <sup>i</sup>BuN<sub>3</sub>, CuI, Na-ascorbate, DMF/H<sub>2</sub>O, r.t.; (h) i—HCl-dioxane, CH<sub>2</sub>Cl<sub>2</sub>, r.t.; ii—BnCOCl or <sup>i</sup>BuCOCl, Et<sub>3</sub>N, CH<sub>2</sub>Cl<sub>2</sub>, r.t.; (i) I<sub>2</sub>, HNO<sub>3</sub>, H<sub>2</sub>SO<sub>4</sub>, AcOH, 80 °C; (j) i—<sup>n</sup>BuLi, CO<sub>2</sub>, THF, -78 °C to r.t.; ii—EDCI, HOBT, DIEA, BnNH<sub>2</sub>, or <sup>i</sup>BuNH<sub>2</sub>, THF, r.t.; (k) i—<sup>n</sup>BuLi, CO<sub>2</sub>, THF, -78 °C to r.t.; ii—K<sub>2</sub>CO<sub>3</sub>, methanol, r.t., 30% in two steps; (l) K<sub>2</sub>CO<sub>3</sub>, MeOH, r.t. AcO: acetate; Bn: benzyl; Bu: butyl; Et: ethyl; <sup>i</sup>Bu: isobutyl; Ph: phenyl; OTf: triflate; r.t.: room temperature; TBS: *tert*-butyldimethylsilyl; TMS: trimethylsilyl; EDCI: 1-(3-dimethylaminopropyl)-3-ethylcarbodiimide hydrochloride; HOBT: 1-hydroxybenzotriazole monohydrate; DIEA: *N,N*-diisopropylethylamine.

irradiation to afford 9,10-diiodo-*m*-carborane **21** in 84% yield. Surprisingly, 5,9,10-triiodo-*m*-carborane **22**, which has not been reported previously, was obtained as a by-product in 10% yield.

The Kumada–Tamao–Corriu cross coupling between **21** and trimethylsilylacetylene was performed under reaction conditions similar to those described in Scheme 2 to give 9,10-bis(trimethylsilyl)acetynyl)-*m*-carborane **23** in 94% yield. After introducing a carboxylic acid into the C1-position of **23**, the resulting carboxylic acid was subjected to amidation reactions with benzyl amine or isobutyl amine using COMU<sup>52</sup> to afford compounds **24a** and **24b** in 41% and 48% yields over two steps, respectively. After removal of the TMS group, the Hüsigen cycloaddition reaction was carried out to obtain compounds **IVa–d** in 29–82% yields over the two steps. Notably, although we were able to synthesize 1,9,10-trisubstituted carboranes, we found it difficult to introduce different substituents at the 9,10-positions of scaffold IV. The structures of **18** (scaffold III), 5,9,10-triiodo-*m*-carborane **22**, and compound **25** (scaffold IV) were determined by X-ray structural analysis.

Finally, the synthesis of 1,2,12-substituted carborane was carried out using *p*-carborane (Scheme 4). The electrophilic iodination at the B2-position of *p*-carborane<sup>50</sup> followed by the Sonogashira–Hagihara cross coupling with propargyl PMB ether produced B2-substituted carborane **26** in 49% yield over two steps. By introducing a hydroxymethyl group into **26** via the lithiation with <sup>n</sup>BuLi followed by the addition to paraformaldehyde, 1,2-disubstituted and 1,7-disubstituted carboranes were generated as regioisomers. After a TBS group was introduced to protect the hydroxy group, a carboxylic acid group was introduced into another carbon atom; subsequently,



**Scheme 4.** Synthesis of scaffold V. Reaction conditions: (a) I<sub>2</sub>, HNO<sub>3</sub>, H<sub>2</sub>SO<sub>4</sub>, AcOH, 80 °C, 99%; (b) propargyl PMB ether, PdCl<sub>2</sub>(PPh<sub>3</sub>)<sub>2</sub>, CuI, toluene, piperidine, 80 °C, 49%; (c) i-<sup>n</sup>BuLi, (CHO)<sub>n</sub>, THF, -78 °C to 0 °C; ii—TBSOTf, 2,6-lutidine, CH<sub>2</sub>Cl<sub>2</sub>, 0 °C to r.t.; iii—<sup>n</sup>BuLi, CO<sub>2</sub>, THF, -78 °C to r.t.; (d) EDCI, HOBT, DIEA, BnNH<sub>2</sub> or <sup>i</sup>BuNH<sub>2</sub>, THF, r.t.; (e) DDQ, NaH<sub>2</sub>PO<sub>4</sub>, CH<sub>2</sub>Cl<sub>2</sub>, H<sub>2</sub>O, r.t.; (f) Dess–Martin periodinane, CH<sub>2</sub>Cl<sub>2</sub>, r.t.; (g) i—NaClO<sub>2</sub>, NaH<sub>2</sub>PO<sub>4</sub>, 2-methyl-2-butene, acetone/H<sub>2</sub>O, r.t.; ii—EDCI, HOBT, DIEA, BnNH<sub>2</sub> or <sup>i</sup>BuNH<sub>2</sub>, THF, r.t.; HCl-dioxane, CH<sub>2</sub>Cl<sub>2</sub>, r.t.; (h) BnCOCl or <sup>i</sup>BuCOCl, Et<sub>3</sub>N, CH<sub>2</sub>Cl<sub>2</sub>, r.t.. AcO: acetate; Bn: benzyl; Bu: butyl; Et: ethyl; <sup>i</sup>Bu: isobutyl; Ph: phenyl; DDQ: 2,3-dichloro-5,6-dicyano-*p*-benzoquinone; PMB: *p*-methoxybenzyl; TBS: *tert*-butyldimethylsilyl; r.t.: room temperature; EDCI: 1-(3-dimethylaminopropyl)-3-ethylcarbodiimide hydrochloride; HOBT: 1-hydroxybenzotriazole monohydrate; DIEA: *N,N*-diisopropylethylamine.

a separation procedure was implemented using preparative HPLC to obtain the 1,7,12-trisubstituted carborane **27** and 1,2,12-trisubstituted carborane **28** in 21% and 16% yields, respectively, over three steps. The carboxylic acids **27** and **28** were subjected to amidation reactions with benzyl amine or isobutyl amine in a manner similar to that described in Scheme 3; subsequently, removal of the PMB group followed by the Dess–Martin oxidation produced aldehydes **31a,b** and **35a,b** in 15–75% yields over three steps. These aldehydes were then subjected to Pinnick–Kraus oxidations, and the resulting carboxylic acids were again subjected to amidation with benzyl amine or isobutyl amine followed by removal of the TBS group to afford **32a–d** and **36a–d** in 55–85% yields over three steps. Finally, esterification with phenylacetyl chloride against methanol gave compounds **Va–p** in 25% to quantitative yields. The absolute structures of the two isomers were confirmed by X-ray crystallography to be **32d** and **36d** (see Scheme 4).

**Biological evaluation of trisubstituted carborane library.** In order to validate the biological activity of the thus synthesized trisubstituted carborane library, we performed cell-based assays to determine: hypoxia

inducible factor (HIF)-1 transcriptional activity, anti-rabies virus activity, and anti-proliferative activity. The experiments designed to determine the prepared carboranes' HIF-1 transcriptional activity were conducted using HeLa cells stably transfected with the hypoxic response element (HRE)-dependent luciferase reporter gene. The cells were incubated in the presence of the various compounds under hypoxic conditions, and fluorescence intensity was recorded to determine the trisubstituted carboranes'  $IC_{50}$  values. The three leucine residues Leu818, Leu819, and Leu822 of the C-terminal helix (helix 3) of HIF-1 $\alpha$  are involved in the PPI between HIF-1 $\alpha$  and p300, which induces transcriptional activity. The anti-rabies virus activity of the synthesized compounds was investigated using N2a cells. N2a cells infected with a recombinant rabies virus expressing *g* luciferase reporter were incubated in the presence of various carboranes. The  $IC_{50}$  values were determined by measuring the luciferase activity in the cell supernatant secreted extracellularly. In addition, since the reporter gene assay was affected by the carboranes' cytotoxicity, cell viability toward both HeLa cells and N2a cells was also measured performing the MTT (3-[4,5-dimethylthiazol-2-yl]-2,5 diphenyl tetrazolium bromide) assay. The results of the said experiments are summarized in Table 1. Among the compounds synthesized, **Vi–m** and **Vo**, characterized by scaffold V, were found to significantly inhibit HIF-1 transcriptional activity ( $IC_{50}$  = 3.24–23.2  $\mu$ M), and carboranes **Iib–g** characterized by scaffold II and carboranes **Va–h** characterized by scaffold V exhibited antiviral activity toward RABV ( $IC_{50}$  = 2.17–8.37  $\mu$ M) and low cytotoxicity toward host cells ( $IC_{50}$  > 30  $\mu$ M). Even though the same substituents had been introduced in the various molecules, the positions of the said substituents dramatically affected the carboranes' biological activities (e.g., see the activities of **Vf** vs. **Vn**). This observation suggests that the protein can strictly recognise the geometrical configuration of substituents. In fact, **IId** with scaffold II and **Vh** with scaffold V exhibited similar antiviral activities, with  $IC_{50}$  values of 3.30 and 4.00  $\mu$ M, respectively. Superimposing the structures of **IId** and **Vh** revealed that three isobutyl groups overlapped completely in each configuration, resulting in similar biological activity (Fig. S1). On the other hand, **IVb** with scaffold IV exhibited high antiviral activity ( $IC_{50}$  = 5.96  $\mu$ M) and a moderate inhibition of HIF-1 transcriptional activity ( $IC_{50}$  = 17.4  $\mu$ M). In order to confirm the possibility of the non-specific effect on the luciferase assay, we selected **Vj**, which showed the most significant inhibition of the HIF-1 transcriptional activity, and examined the direct luciferase inhibition test<sup>53</sup>. As shown in Fig. S2, **Vj** did not inhibit luciferase itself, indicating that inhibitions by compounds demonstrated in Table 1 were not caused by a non-specific effect on the luciferase assay. We also examined the effects of compounds **Vo**, **Vi**, **Vj**, and **Vk** on protein levels of HIF-1 $\alpha$  and CA9 downstream of HIF-1 $\alpha$  under hypoxia, and found that the protein levels of HIF-1 $\alpha$  treated with the compounds were similar to that of control, whereas the suppression of the protein levels of CA9 were observed in the cells treated with the compounds, and the CA9 mRNA significantly suppressed by **Vk** under hypoxia. These results suggest that the compounds inhibit the HIF-1 $\alpha$ -induced transcriptional pathway without affecting the HIF-1 $\alpha$  protein expression (Fig. S3).

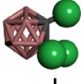


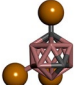

Furthermore, to our surprise, **Vi–l**, **Vo**, and **Vp** were found to stimulate the proliferation of the rabies virus. These compounds are the first to have ever been found to activate the said process. In fact, even a carborane with the same scaffold, compound **Va**, exhibited significant antiviral activity ( $IC_{50}$  = 3.87  $\mu$ M), whereas **Vi** activated the proliferation of the rabies virus (Fig. 2). Notably compounds **Va** and **Vi** comprise the same substituents (Bn groups). A similar divergence of activity was observed between compounds **Va–h** and compounds **Vi–p**. In addition, the intracellular viral protein accumulation and the virus titer were measured using **Vp**. As shown in Fig. S4, the intracellular viral proteins treated with **Vp** was significantly increased without affecting the virus titer. Since viral ribonucleoproteins (RNPs) are formed from the replicated genomic RNA and Rabies N proteins are released from the cell to infecting other cells<sup>54</sup>, these results suggest that **Vp** may have inhibited the formation of viral ribonucleoproteins, resulting in increased accumulation of viral proteins in the cell.

The compound concentration required to inhibit the relative light units by 50% ( $IC_{50}$ ) was determined based on semi-logarithmic dose–response plots. All the samples were tested in triplicate. [a] YC-1 was used as positive control with  $IC_{50}$  of 0.17  $\mu$ M. [b] Favipiravir was used as a control with  $IC_{50}$  of 38  $\mu$ M.

**Assessment of trisubstituted carboranes for comprehensive chemical space search.** Finally, we investigated the morphologies of the herein synthesized compounds using the normalized principal moment of inertia (PMI)<sup>55</sup>, which is an approach commonly employed to assess the molecular shape of compound libraries in comparison to 2-butyne (rod), benzene (disc), and adamantane (sphere). For all compounds, 25 conformations were generated in each compound using the 'iCon fast' option of LigandScout 4.4, and the normalized PMI values calculated with the aid of the RDKit<sup>56</sup> were plotted (Fig. 3; see also Fig. S5). Notably, a higher number of compounds characterized by scaffolds I and II (green and blue dots in Fig. 3) occupies the sphere-like shape section of the graph in Fig. 3 than compounds characterized by other scaffolds. On the other hand, compounds characterized by scaffold V tended to occupy the rod–disc area of the graph, as a result of the presence of the two substituents in para positions to each other aligned in a linear fashion. Scaffold III and IV-based compounds, derived from *m*-carborane, occupied the middle section of the morphology graph. The results of the PMI analysis indicate, therefore, that the herein synthesized carboranes characterized by scaffolds I–V cover all the regions of the described three-dimensional shape space.

## Conclusion

We successfully synthesized a total of 42 trisubstituted carboranes characterized by five basic scaffolds that were found to occupy the entire rod–disc–sphere chemical morphology space; we achieved this goal by exploiting the different reactivities of the twelve vertices of *o*-, *m*-, and *p*-carboranes. The typical three-dimensional structures of each scaffold type of trisubstituted carboranes, **4**, **14**, **18**, **25**, **32d**, and **36d**, were unambiguously determined by X-ray structural analysis. The synthesized compounds were utilized in cell-based biological assays performed to determine the effects of various carboranes on HIF-1 transcriptional activity and anti-rabies virus activity.

Scaffold	Compound	HIF-1 <sup>[a]</sup>	RABV <sup>[b]</sup>	HeLa cells	N2a cells
 I	Ia	> 30	> 9	> 30	> 30
	Ib	> 30	> 9	> 30	> 30
	Ic	> 30	> 9	> 30	> 30
	Id	> 30	> 9	> 30	> 30
	Ie	> 30	> 9	> 30	> 30
	If	> 30	> 9	> 30	> 30
 II	IIa	> 30	> 9	> 30	> 30
	IIb	> 30	5.74	> 30	> 30
	IIc	> 30	6.87	> 30	> 30
	IId	> 30	3.30	> 30	> 30
	IIe	> 30	8.14	> 30	> 30
	IIf	> 30	5.78	> 30	> 30
	IIg	> 30	8.37	> 30	> 30
	IIh	> 30	> 9	> 30	> 30
 III	IIIa	> 30	> 9	> 30	> 30
	IIIb	26.3	> 9	> 30	> 30
	IIIc	> 30	> 9	> 30	> 30
	IIId	23.0	> 9	> 30	> 30
	IIIe	> 30	> 9	> 30	> 30
	IIIf	> 30	> 9	> 30	> 30
	IIIg	> 30	> 9	> 30	> 30
	IIIh	> 30	> 9	> 30	> 30
 IV	IVa	> 30	> 9	> 30	> 30
	IVb	17.4	5.96	> 30	> 30
	IVc	> 30	> 30	> 30	> 30
	IVd	> 30	> 30	> 30	> 30
 V	Va	> 30	3.87	> 30	> 30
	Vb	> 30	2.17	> 30	> 30
	Vc	> 30	4.44	> 30	> 30
	Vd	> 30	3.95	> 30	> 30
	Ve	> 30	3.46	> 30	> 30
	Vf	> 30	2.56	> 30	> 30
	Vg	> 30	5.08	> 30	> 30
	Vh	> 30	4.00	> 30	> 30
	Vi	5.46	Activation	16.7	> 30
	Vj	3.24	Activation	> 30	22.6
	Vk	3.64	Activation	15.0	21.2
	VI	18.1	Activation	21.7	25.2
	Vm	23.2	> 9	> 30	> 30
	Vn	> 30	> 9	> 30	> 30
	Vo	9.21	Activation	20.9	7.90
	Vp	> 30	Activation	> 30	8.00

**Table 1.** Results of the evaluation of the biological activities of various members of the trisubstituted carborane compound library. The compound concentration required to inhibit the relative light units by 50% (IC<sub>50</sub>) was determined based on semi-logarithmic dose–response plots. All the samples were tested in triplicate. <sup>[a]</sup> YC-1 was used as positive control with IC<sub>50</sub> of 0.17 μM. <sup>[b]</sup> Favipiravir was used as a control with IC<sub>50</sub> of 38 μM.



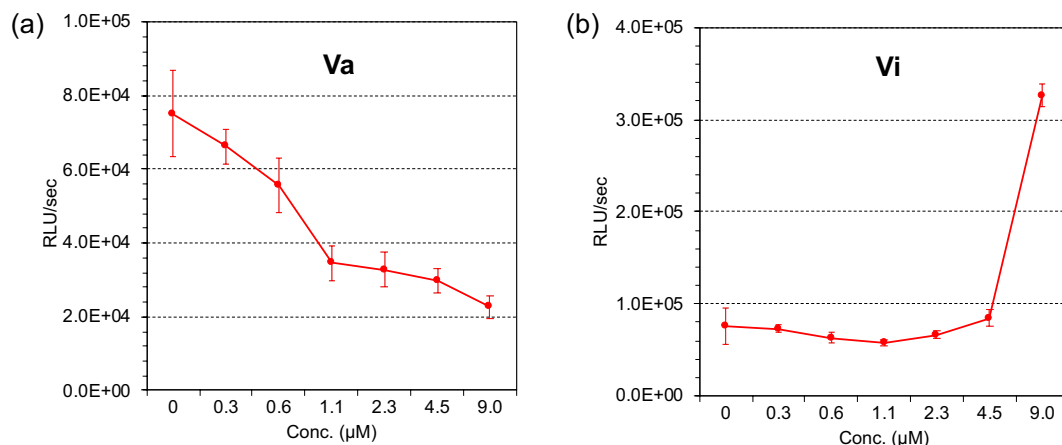


**Figure 2.** Compound concentration-dependent effects on the proliferation of the rabies virus: (a) Antiviral activity of Va and (b) activation of rabies virus proliferation by Vi. Compound concentration is reported on the x axis and fluorescent intensity on the y axis.

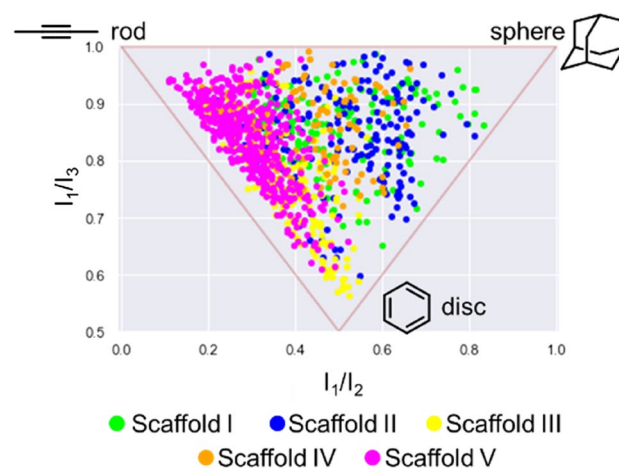


**Figure 3.** Normalized principal moment of inertia analysis of members of the synthesized trisubstituted carborane library; parameters  $I_1/I_2$  and  $I_1/I_3$  were defined by Sauer and Schwartz<sup>53</sup>. These values were calculated with the aid of RDKit<sup>54</sup>.

Compounds characterized by scaffold V (e.g., **Vi–m**, and **Vo**) were mainly observed to exhibit significant inhibition of HIF-1 transcriptional; by contrast, anti-rabies virus activity was observed not only for compounds with scaffold V (compounds **Va–h**) but also for carboranes with scaffold II (compounds **Ib–g**) and IV (compound **Iv**). The pharmacophore model predicted by the scaffold V carboranes, which exhibited significant anti-rabies virus activities, agreed well especially with compounds **Ib** and **Id** with scaffold **Iv** and compound **Iv** with scaffold IV. Furthermore, the first compounds to have ever been found to stimulate the proliferation of the rabies virus were identified in the present study, and they were determined to be scaffold V compounds. Therefore, we believe that our strategy for the systematic design of three-dimensionally divergent molecules based on five different types of trisubstituted carboranes has great potential to satisfy all directions in the chemical space and to afford the identification of novel biologically active molecules that have not been recognised by other drug discovery approaches.

## Experimental section

**Synthesis of trisubstituted carboranes.** The synthetic procedures and characterization were provided in “Supplementary information S1”.

**X-ray crystallography.** All data generated or analyzed were provided in “Supplementary information S1”. CCDC 2110331, 2110336–2110341.

**Cell culture.** Human epithelioid cervical carcinoma (HeLa) cells were obtained from the Cell Resource Center for Biomedical Research, Institute of Development, Aging and Cancer, Tohoku University (Sendai, Japan). The cells were incubated with RPMI-1640 medium (FUJIFILM Wako Pure Chemical) containing 10% fetal bovine serum (Gibco; Thermo Fisher Scientific) and 1% penicillin/streptomycin (FUJIFILM Wako Pure Chemical). Cells were incubated in a cell incubator with 5% CO<sub>2</sub> at 37 °C. Neuro 2a (N2a) cells were incubated with D-MEM medium (FUJIFILM Wako Pure Chemical) containing 10% fetal bovine serum (Gibco; Thermo Fisher Scientific) and 1% penicillin/streptomycin (FUJIFILM Wako Pure Chemical). Cells were incubated in a cell incubator with 5% CO<sub>2</sub> at 37 °C.

**MTT assay.** HeLa cells or N2a cells (5 × 10<sup>3</sup> cells per well of a 96-well plate) were incubated under 5% CO<sub>2</sub> at 37 °C in RPMI-1640 media (for HeLa cells) or D-MEM media (for N2a cells) containing 10% fetal bovine serum, 1% penicillin/streptomycin, and various concentrations of compound (10 mM in DMSO) for 72 h. After the incubation, 3'-(4,5-dimethylthiazole-2-yl)-2,5-diphenyltetrazolium bromide (MTT) in PBS (5 mg/mL, 10 μL) were added, and the cells were further incubated at 37 °C for 2 h. After removal of the medium, DMSO (100 μL) was added and the absorbance at 590 nm was measured with a microplate reader. The IC<sub>50</sub> value was determined from semilogarithmic dose–response plots.

**Luciferase reporter gene assay for HIF transcriptional activity.** HeLa cells transfected with hypoxia response element dependent firefly luciferase reporter construct (HRE-Luc) were seeded in a 96-well plate (2.5 × 10<sup>4</sup> cells per a well) and incubated for 6 h under 5% CO<sub>2</sub> at 37 °C with RPMI-1640 media containing 10% fetal bovine serum, 1% penicillin/streptomycin. After the incubation, cells were treated with various concentration of compound (10 mM in DMSO) and incubated at the same condition for 1 h. Then the cells were incubated at normoxic condition (1% O<sub>2</sub>, 5% CO<sub>2</sub>, 37 °C) for 12 h. At the same time, cells without compounds were incubated at hypoxic condition for 12 h. After removal of the media cells were washed with PBS and the luciferase reporter gene assay was performed with Luciferase Assay System (Promega, Madison, WI, USA) according to the manufacturer's instructions. The compound concentration required to reduce relative luminescence units (RLU) by 50% (IC<sub>50</sub>) was determined from semilogarithmic dose response plots.

**Luciferase reporter gene assay for antiviral activity against rabies virus.** The recombinant rabies virus strain 1088 expressing gaussia luciferase (1088/GLuc) was generated as described previously<sup>4</sup>. The virus titer was determined using focus assay as reported<sup>5</sup> and expressed as focus forming units (FFU). N2a cells (4 × 10<sup>4</sup> cells per well) and 1088/GLuc (4 × 10<sup>2</sup> FFU per well) were prepared in E-MEM containing 10% fetal bovine serum and antibiotics, and the mixed solution was applied to a 96-well black plate with clear bottoms (Greiner). Subsequently, various concentrations of compounds were prepared in the medium and added to each well. The microplates were incubated at 37 °C under 5% CO<sub>2</sub> for 3 days, and then, a luciferase reporter gene assay was performed using Pierce Gaussia Luciferase Glow Assay Kit (Thermo Fisher Scientific). The substrate solution was added to each well, and RLU was immediately measured using a microplate luminometer LuMate (Awareness Technology). Based on the RLU value, IC<sub>50</sub> was determined from semilogarithmic dose–response plots.

Received: 7 October 2021; Accepted: 24 November 2021

Published online: 16 December 2021

## References

- Odling-smee, L. & Dobson, C. M. Insight chemical space and biology. *Nature* **432**, 824–828 (2004).
- Barker, A., Kettle, J. G., Nowak, T. & Pease, J. E. Expanding medicinal chemistry space. *Drug Discov. Today* **18**, 298–304 (2013).
- Butler, M. S. Natural products to drugs: Natural product derived compounds in clinical trials. *Nat. Prod. Rep.* **22**, 162–195 (2005).
- Newman, D. J. & Cragg, G. M. Natural products as sources of new drugs over the last 25 years. *J. Nat. Prod.* **70**, 461–477 (2007).
- Newman, D. J. & Cragg, G. M. Natural products as sources of new drugs from 1981 to 2014. *J. Nat. Prod.* **79**, 629–661 (2016).
- Lovering, F., Bikker, J. & Humblet, C. Escape from flatland: Increasing saturation as an approach to improving clinical success. *J. Med. Chem.* **52**, 6752–6756 (2009).
- Lovering, F. Escape from Flatland 2: Complexity and promiscuity. *Medchemcomm* **4**, 515–519 (2013).
- Tajabadi, F. M. *et al.* Design and synthesis of natural product inspired libraries based on the three-dimensional (3D) cedrane scaffold: Toward the exploration of 3D biological space. *J. Med. Chem.* **61**, 6609–6628 (2018).
- Schreiber, S. L. Target-oriented and diversity-oriented organic synthesis in drug discovery. *Science* **287**, 1964–1969 (2000).
- Schreiber, S. L. Molecular diversity by design. *Nature* **457**, 153–154 (2009).
- Galloway, W. R. J. D., Isidro-Llobet, A. & Spring, D. R. Diversity-oriented synthesis as a tool for the discovery of novel biologically active small molecules. *Nat. Commun.* **1**, 1–13 (2010).
- Kopp, F., Stratton, C. F., Akella, L. B. & Tan, D. S. A diversity-oriented synthesis approach to macrocycles via oxidative ring expansion. *Nat. Chem. Biol.* **8**, 358–365 (2012).
- Beckmann, H. S. G. *et al.* A strategy for the diversity-oriented synthesis of macrocyclic scaffolds using multidimensional coupling. *Nat. Chem.* **5**, 861–867 (2013).
- Kim, J. *et al.* Diversity-oriented synthetic strategy for developing a chemical modulator of protein–protein interaction. *Nat. Commun.* **7**, 1–10 (2016).
- Bregadze, V. I. Dicarba-closo-dodecaboranes C<sub>2</sub>B<sub>10</sub>H<sub>12</sub> and their derivatives. *Chem. Rev.* **92**, 209–223 (1992).
- Issa, F., Kassiou, M., Rendina, L. M. & Rendina, M. Boron in drug discovery: Carboranes as unique pharmacophores in biologically active compounds. *Chem. Rev.* **111**, 5701–5722 (2011).
- Endo, Y. *et al.* Dicarba-closo-dodecaboranes as a pharmacophore. Novel potent retinoid agonists. *Chem. Pharm. Bull.* **47**, 585–587 (1999).

18. Scholz, M. & Hey-Hawkins, E. Carboranes as pharmacophores: Properties, synthesis, and application strategies. *Chem. Rev.* **111**, 7035–7062 (2011).
19. Leśnikowski, Z. J. Challenges and opportunities for the application of boron clusters in drug design. *J. Med. Chem.* **59**, 7738–7758 (2016).
20. Stockmann, P., Gozzi, M., Kuhnert, R., Sárosi, M. B. & Hey-Hawkins, E. New keys for old locks: Carborane-containing drugs as platforms for mechanism-based therapies. *Chem. Soc. Rev.* **48**, 3497–3512 (2019).
21. Endo, Y. *et al.* Potent estrogen agonists based on carborane as a hydrophobic skeletal structure: A new medicinal application of boron clusters. *Chem. Biol.* **8**, 341–355 (2001).
22. Reynolds, R. C. *et al.* Novel boron-containing, nonclassical antifolates: Synthesis and preliminary biological and structural evaluation. *J. Med. Chem.* **50**, 3283–3289 (2007).
23. Shimizu, K. *et al.* Boron-containing phenoxyacetanilide derivatives as hypoxia-inducible factor (HIF)-1 $\alpha$  inhibitors. *Bioorg. Med. Chem. Lett.* **20**, 1453–1456 (2010).
24. Ban, H. S., Shimizu, K., Minegishi, H. & Nakamura, H. Identification of HSP60 as a primary target of *o*-carboranylphenoxyacetanilide, an HIF-1 $\alpha$  Inhibitor. *J. Am. Chem. Soc.* **132**, 11870–11871 (2010).
25. Julius, R. L. *et al.* Synthesis and evaluation of transthyretin amyloidosis inhibitors containing carborane pharmacophores. *Proc. Natl. Acad. Sci. USA* **104**, 4808–4813 (2007).
26. Neumann, W. *et al.* Nido-dicarbaborate induces potent and selective inhibition of cyclooxygenase-2. *ChemMedChem* **11**, 175–178 (2016).
27. Fujii, S. *et al.* Boron cluster-based development of potent nonsteroidal vitamin D receptor ligands: Direct observation of hydrophobic interaction between protein surface and carborane. *J. Am. Chem. Soc.* **133**, 20933–20941 (2011).
28. Otero, R. *et al.* Carborane-based design of a potent vitamin D receptor agonist. *Chem. Sci.* **7**, 1033–1037 (2016).
29. Lee, M. W., Sevryugina, Y. V., Khan, A. & Ye, S. Q. Carboranes increase the potency of small molecule inhibitors of nicotinamide phosphoribosyltransferase. *J. Med. Chem.* **55**, 7290–7294 (2012).
30. Asawa, Y. *et al.* Structure-based drug design of novel carborane-containing nicotinamide phosphoribosyltransferase inhibitors. *Bioorg. Med. Chem.* **27**, 2832–2844 (2019).
31. Quan, Y. & Xie, Z. Controlled functionalization of *o*-carborane via transition metal catalyzed B-H activation. *Chem. Soc. Rev.* **48**, 3660–3673 (2019).
32. Au, Y. K. & Xie, Z. Recent advances in transition metal-catalyzed selective B-H functionalization of *o*-carboranes. *Bull. Chem. Soc. Jpn.* **94**, 879–899 (2021).
33. Ueda, H., Yoshimori, A. & Nakamura, H. Discovery of bicyclo [3, 3, 1] non-2-ene as a novel skeleton for HIF-1 inhibitors. *Bioorg. Med. Chem.* **26**, 3345–3351 (2018).
34. Umedera, K. *et al.* Synthesis of three-dimensional (3D) (Di)azatricyclododecene scaffold and its application to peptidomimetics. *Chem. A Eur. J.* **27**, 11888–11894 (2021).
35. Shimizu, T. *et al.* Design and synthesis of 14 and 15-membered macrocyclic scaffolds exhibiting inhibitory activities of hypoxia-inducible factor 1 $\alpha$ . *Bioorganic Med. Chem.* **30**, 115949 (2021).
36. Jones, S. & Thornton, J. M. Review principles of protein–protein interactions. *Proc. Natl. Acad. Sci. USA* **93**, 13–20 (1996).
37. Azzarito, V., Long, K., Murphy, N. S. & Wilson, A. J. Inhibition of  $\alpha$ -helix-mediated protein–protein interactions using designed molecules. *Nat. Chem.* **5**, 161–173 (2013).
38. Pelay-Gimeno, M., Glas, A., Koch, O. & Grossmann, T. N. Structure-based design of inhibitors of protein–protein interactions: Mimicking peptide binding epitopes. *Angew. Chemie Int. Ed.* **54**, 8896–8927 (2015).
39. Mabonga, L. & Kappo, A. P. Peptidomimetics: A synthetic tool for inhibiting protein–protein interactions in cancer. *Int. J. Pept. Res. Ther.* **26**, 225–241 (2020).
40. Adams, J. *et al.* Proteasome inhibitors: A novel class of potent and effective antitumor agents. *Cancer Res.* **59**, 2615–2622 (1999).
41. Cheng, A. C. *et al.* Structure-based maximal affinity model predicts small-molecule druggability. *Nat. Biotechnol.* **25**, 71–75 (2007).
42. Souers, A. J. *et al.* ABT-199, a potent and selective BCL-2 inhibitor, achieves antitumor activity while sparing platelets. *Nat. Med.* **19**, 202–208 (2013).
43. Sattler, M. *et al.* Structure of Bcl-x(L)-Bak peptide complex: Recognition between regulators of apoptosis. *Science* **275**, 983–986 (1997).
44. Croce, C. M. & Reed, J. C. Finally, an apoptosis-targeting therapeutic for cancer. *Cancer Res.* **76**, 5914–5920 (2016).
45. Bruncko, M. *et al.* Studies leading to potent, dual inhibitors of Bcl-2 and Bcl-xL. *J. Med. Chem.* **50**, 641–662 (2007).
46. Arkin, M. M. R. & Wells, J. A. Small-molecule inhibitors of protein–protein interactions: Progressing towards the dream. *Nat. Rev. Drug Discov.* **3**, 301–317 (2004).
47. Tošovská, P. & Arora, P. S. Oligoioxopiperazines as nonpeptidic  $\alpha$ -helix mimetics. *Org. Lett.* **12**, 1588–1591 (2010).
48. Yan, C., Wu, F., Jernigan, R. L., Dobbs, D. & Honavar, V. Characterization of protein–protein interfaces. *Protein J.* **27**, 59–70 (2008).
49. Wingen, L. M. & Scholz, M. S. B-Cyanodicarba-*closo*-dodecaboranes: Facile synthesis and spectroscopic features. *Inorg. Chem.* **55**, 8274–8276 (2016).
50. Himmelspach, A. & Finze, M. Dicarba-*closo*-dodecaboranes with one and two ethynyl groups bonded to boron. *Eur. J. Inorg. Chem.* **10**, 2012–2024 (2010).
51. Minegishi, H., Matsukawa, T. & Nakamura, H. Synthesis and biological evaluation of diaryl-substituted carboranes as inhibitors of hypoxia inducible factor (HIF)-1 transcriptional activity. *ChemMedChem* **8**, 265–271 (2013).
52. Scholz, M. S. & Wingen, L. M. Synthesis of Dicarba-*closo*-dodecaborane-1-carboxamides. *Inorg. Chem.* **56**, 5510–5513 (2017).
53. Fuse, S. *et al.* Design, synthesis, and evaluation of indeno[2,1-*c*]pyrazolones for use as inhibitors against hypoxia-inducible factor (HIF)-1 transcriptional activity. *Bioorg. Med. Chem.* **28**, 115207 (2020).
54. Lahaye, X. *et al.* Functional characterization of Negribodies (NBs) in rabies virus-infected cells: Evidence that NBs are sites of viral transcription and replication. *J. Virol.* **83**, 7948–7958 (2009).
55. Sauer, W. H. B. & Schwarz, M. K. Molecular shape diversity of combinatorial libraries: A prerequisite for broad bioactivity. *J. Chem. Inf. Comput. Sci.* **43**, 987–1003 (2003).
56. RDKit: Cheminformatics and machine learning software (2013). <http://www.rdkit.org>. Accessed 7 Dec 2021.

## Acknowledgements

We thank Dr. Yoshihisa Sei (Technical Department, Tokyo Institute of Technology) for his technical assistance with X-ray crystallographic analysis. This work was partially supported by the Ministry of Education, Science, Sports and Culture, Grants-in-Aid for “Chemistry for Multimolecular Crowding Biosystems (20H04699 to H.N.)” and for JSPS Fellows (ID No. 21J13988 to Y. A.).

## Author contributions

Y.A. and S.H. synthesized the compounds, evaluated inhibitory activity toward HIF-1 $\alpha$  and cytotoxicity, and analysed data. Y.A. and A.Y. performed computational analysis of the compounds. K.Y. and A.K. evaluated inhibitory activity toward RABV. H.N. and H.K. supervised the whole project. Y.A. and H.N. wrote the manuscript.

### Competing interests

The authors declare no competing interests.

### Additional information

**Supplementary Information** The online version contains supplementary material available at <https://doi.org/10.1038/s41598-021-03459-6>.

**Correspondence** and requests for materials should be addressed to H.N.

**Reprints and permissions information** is available at [www.nature.com/reprints](http://www.nature.com/reprints).

**Publisher's note** Springer Nature remains neutral with regard to jurisdictional claims in published maps and institutional affiliations.



**Open Access** This article is licensed under a Creative Commons Attribution 4.0 International License, which permits use, sharing, adaptation, distribution and reproduction in any medium or format, as long as you give appropriate credit to the original author(s) and the source, provide a link to the Creative Commons licence, and indicate if changes were made. The images or other third party material in this article are included in the article's Creative Commons licence, unless indicated otherwise in a credit line to the material. If material is not included in the article's Creative Commons licence and your intended use is not permitted by statutory regulation or exceeds the permitted use, you will need to obtain permission directly from the copyright holder. To view a copy of this licence, visit <http://creativecommons.org/licenses/by/4.0/>.

© The Author(s) 2021